End Group Effects on Surface Properties of Polymers: Semiempirical Calculations and Comparison to Experimental Surface Tensions for α,ω-Functional Poly(dimethylsiloxanes)

Claire Jalbert[†] and Jeffrey T. Koberstein*[,‡]

The Polymer Program and Department of Chemical Engineering, Institute of Materials Science, University of Connecticut, Storrs, Connecticut 06269-3136

Arvind Hariharan[§] and Sanat K. Kumar[||]

Department of Materials Science and Engineering, Pennsylvania State University, University Park, Pennsylvania 16802

Received February 13, 1996; Revised Manuscript Received May 2, 1997[⊗]

ABSTRACT: Current theoretical models for the surface behavior of polymers have stressed the importance of several factors such as the chain length (r), local chain stiffness, and the surface energy difference between chain ends and middle segments, χ_s. Here we assert that the critical parameter, which is affected by all of these factors, that controls thermodynamic properties is the surface composition of the different moieties in the macromolecular system. Composite surface properties, such as the surface tension, are calculated directly by assuming that the end group and repeat unit segments contribute to surface properties weighted by the composition in the lattice layer, which is immediately adjacent to the surface. We utilize the Scheutjens−Fleer lattice self-consistent mean-field model and Monte Carlo simulations to determine the surface composition of end groups for end-functionalized polymer chains. We find that end group segregation is primarily controlled by surface energetic differences between the chain ends and chain middle moieties and that entropic effects are effectively irrelevant in this context. Within the range of surface energy differences that are expected to be encountered in practice, the predicted surface segregation of chain ends is so small that the molecular weight dependence of the surface tension of an end-functionalized polymer melt is for all practical purposes determined by the direct relationship between the bulk end group concentration and chain length represented by $\phi_e = 2/r$. Group contribution methods are employed to estimate the surface tensions of the end and middle groups, and no adjustable parameters are required. The simple model provides a facile method for determining the variation of surface tension with molecular weight and end group type and reproduces well experimental surface tension data for several α,ω-functional poly(dimethylsiloxanes).

I. Introduction

The surface and interfacial behavior of polymers are key to their performance in a variety of applications. For example, the surface tension of a polymer melt controls its wetting behavior on a substrate and is also critical in determining the mechanical strength of the resultant polymer/substrate composite interface.[1,2] It has been generally believed, on the basis of the Poser−Sanchez theory, that the main factor in determining the surface tensions of polymer systems is the bulk density of the condensed polymer phase.[3] While this result therefore appears to validate a corresponding states principle for this important surface property,[4−7] there exist important exceptions to this rule. For example, Koberstein and co-workers[8] have considered α,ω-functional poly(dimethylsiloxanes) (PDMS) terminated with amine groups and found that, while the bulk densities of these materials increased with increasing chain length, the surface tension showed the opposite chain length dependence. The understanding of the role of end groups in this departure from the generally valid corresponding states principle for surface tensions constitutes the focus of this paper.

We shall show here that the surface tensions of end functionalized chains, γ, can be described by the simple equation

$$\gamma = \frac{2}{r}\gamma_e + \left(1 - \frac{2}{r}\right)\gamma_m \tag{1}$$

where r is the chain length of the polymer (see eq 2 for definition) and γ_e and γ_m, which are the surface tensions of the end groups and middle moieties, respectively, can be obtained from group contribution methods. These results suggest that the surface segregation of chain ends, which will be shown to be driven primarily by surface energy differences between end groups and middle moieties, as well as any entropic effects, do not play primary roles in determining the surface tension. These conclusions will be illustrated conclusively in this manuscript.

It has been well-known for sometime[9−12] that, even in the case of athermal systems near neutral walls, the end groups from a polymer chain partition preferentially to the surface because this results in a smaller loss of conformational entropy for the system. This entropic driving force, however, is generally coupled to energetic effects[13] and previous work has demonstrated that the end groups of a polymer chain, which are chemically distinct from the repeat unit segments, could be preferentially partitioned to or away from a surface depending on the value of χ_s, the dimensionless surface energy difference between an end and repeat unit segment.[14,15]

Two different theoretical approaches have been adopted to explore the surface properties, especially

[†] Current address: 3M Center, Bldg. 201-3E-03, St. Paul, MN 55144-1000.
[‡] E-mail address: jeff@mail.ims.uconn.edu.
[§] Current address: Bankers Trust Corp., 130 Liberty St., New York, NY 10006.
[||] E-mail address: kumar@plmsc.psu.edu.
[⊗] Abstract published in *Advance ACS Abstracts,* July 1, 1997.

S0024-9297(96)00224-0 CCC: $14.00

surface tensions, of polymer melts as a function of molecular weight. A successful treatment for the surface tensions of melts and blends[5−7] involves the use of the Cahn−Hilliard model as suggested by Poser and Sanchez.[3] While this method provides a direct connection between the density (or equation of state) of a polymer system and its surface tension, the major drawback of this model is that it does not account explicitly for chain architecture and hence cannot account for the segregation of specific chain moieties to the surface. This method, therefore, cannot be used to predict accurately the role of end groups on the surface properties of end-functional polymer systems[8].

In contrast to this approach, Theodorou[16] has extended the lattice self-consistent mean-field model of Scheutjens and Fleer[2] so as to be applicable to the behavior of copolymers with arbitrary architecture near a hard surface. Specific information that results from this formalism includes the conformations of macromolecules in the interface, as well as the segregation of specific chain moieties to the surface. Thermodynamic information, such as surface tensions, can also be enumerated through this approach. This methodology, in principle, therefore overcomes the deficiencies of the Cahn−Hilliard calculations discussed above. An important point about the specific implementation of Theodorou is that the polymer system, which was considered near a hard wall, was modeled as incompressible, and hence the total polymer density was constant everywhere in the system. However, the densities of the different moieties could have gradients, such as those driven by the surface segregation of specific chain groups, as long as they satisfied this overall constraint. Consequently, while this model did not include the effects of the large density gradients present near the free surface it nevertheless incorporated the effects of chain architecture on the surface tension of an incompressible model. The extension of this model to the case of the air−polymer interface has been performed recently by Hariharan and Harris[17,18] and by Theodorou,[19] and it has been shown that the predicted surface tension not only is a consequence of the large density gradient at the air interface as modeled in the work of Poser and Sanchez[3] but also is due to the conformational effects incorporated in the lattice work of Theodorou. Both of these factors have to be properly modeled if an accurate measure of the surface tension of this multiconstituent polymer system is to be obtained.

There are two important facts that need to be stressed in this context. First, although the calculations of Hariharan and Harris[17] account for the sharp density gradient near the free surface, these computations tend to be numerically unstable and are therefore cumbersome to perform on a routine basis. Second, it has been found that the predicted surface segregation of chain ends is only slightly affected by the incorporation of the large density gradients in the vicinity of the air surface.[20] Based on these two facts we employ herein the Scheutjens−Fleer mean-field lattice model in the incompressible limit to determine the segregation of end groups to the surface. The only parameters needed to perform these calculations are the chain length of the polymer and the surface energy difference between the chain ends and middle moieties, which was obtained from group contribution methods. In order to reproduce the appropriate bulk density, we employ a normalized chain length given by the volume of the polymer chain divided by the volume of the end group segment. It is further assumed that all of the effects arising from the sharp density gradients at the air surface are built into the group contribution values for the surface tensions of the two different segments. We find that the surface segregation of chain ends is primarily dominated by energetic effects and that entropic effects do not play a significant role in this context. The surface tensions of end-functional polymer melts can be calculated as a function of molecular weight by adding the surface tensions of the ends and middle moieties, weighted by the surface composition determined by the mean-field theory. This approach is compared in its predictive power with an even simpler model where the surface composition is directly determined by chain molecular weight, i.e., $\phi_e = 2/r$. Since both of these methods provide remarkable descriptions of the recent experimental measurements of the surface tensions of α,ω-functional poly(dimethysiloxane) (PDMS) melts, we conclude that these simple ideas embody the essence of this physical situation.

The remainder of this paper is organized as follows. In section 2 we briefly review the theoretical approaches utilized in this paper. Section 3 discusses the structural properties and surface tensions derived for end-functional polymer chains in the framework of this approximate model. Section 4 contains our primary conclusions, while a discussion of off-lattice Monte Carlo simulations, which complement the lattice calculations, are deferred to Appendix A. Details regarding group contribution calculations are contained in Appendix B, and a procedure for interpolating the theoretical results is presented in Appendix C.

II. Theory

II.1. Analytical Model. The analytical model utilized in this work is the mean-field self-consistent lattice theory of Scheutjens and Fleer[2] as extended to the case of copolymers with arbitrary architectures by Theodorou.[16,17] We summarize a few salient features of the model here and refer the interested reader to published work.[16,21]

Space is discretized into a cubic lattice with layers parallel to two impenetrable surfaces that sandwich the homopolymer film. In the current manifestation, the lattice volume is set equal to the volume of the end group and the number of total chain segments, or normalized chain length, r, is calculated as the total volume of the chain divided by the volume of the end group

$$r = \frac{(Zv_r + 2v_e)}{v_e} \tag{2}$$

where Z is the polymerization index, v_r is the volume of the repeat unit, and v_e is the volume of the end group. The two walls are typically separated by a large enough distance that a bulklike region exists in the center of the film. Properties are symmetric about the center of the film since the two walls are defined to be identical. An incompressible system is considered, and in the framework of the model this implies that each lattice site is occupied exactly once by a chain segment.[16,21] The chain architecture considered here is that of a triblock copolymer with the two outer blocks occupying exactly one lattice site each.

The bulk interaction parameter,[22] χ, between an end group and a middle moiety is assumed, for the sake of

simplicity, to be equal to zero. While this assumption is not expected to seriously alter findings when χ is small, the theoretical results may not be quantitatively reliable for cases where χ is large, therefore necessitating extensions to the theory as proposed by Hariharan and Harris.[17] This extension, however, is not considered in this work where the bulk thermodynamic corresponds to an athermal triblock copolymer that, consequently, will not undergo microphase separation.

The only interaction parameter in the system is the dimensionless surface energy difference parameter between an end group and a repeat unit segment,

$$\chi_s = \frac{U_s^1 - U_s^2}{k_B T} \tag{3}$$

where k_B is Boltzmann's constant, T is the temperature, and U_s^i is defined as,

$$U_s^i \equiv \omega_{is} - \frac{1}{2}\omega_{ii} \tag{4}$$

Here ω_{is} is the energy of interaction between a segment of type i and the surface, and ω_{ii} is the energy of interaction between two i segments. The quantity, U_s^i, consequently, defines the change in energy associated with moving a segment of type i from the pure bulk state to the surface. If we now denote the two end group segments on each chain as component 1 and the repeat unit segments as component 2, respectively, then a positive value of χ_s implies that end groups are repelled from the surface, while a negative value implies that the chain ends are preferentially adsorbed at the surface.

The formalism then involves the construction of the grand potential for this system,[16,21] which is a functional of the density profile of either the repeat unit or the end group segments. Note that the incompressibility condition requires that the end group and repeat unit segment densities in each layer must sum to unity. The density profiles of the end groups result when this grand potential is minimized subject to the incompressibility constraint. Quantities including the structure of the molecules as characterized by their order parameters, chain shapes, etc., as well as thermodynamic properties such as surface tension, then result naturally from this formalism.

II.2. Monte Carlo Simulations. In conjunction with the lattice calculations we have also performed Monte Carlo simulations for end-functional polymer chains. While the reader is referred to Appendix A for more details of the simulation method and results, the essential feature of this model is that, since we deal with an off-lattice system, the condition of literal incompressibility that is assumed in the lattice calculations cannot be imposed. Further, the bulk interaction parameter between the end and middle segments has been set to zero as in the case of the lattice calculations. The results from the lattice calculations are then compared to the simulations in Appendix A so as to comment on the effects of various approximations in the analytical calculations on the structure of these model polymer chains in the interface. We find qualitative agreement in all cases, suggesting that the Scheutjens−Fleer mean-field theory provides a reliable description of the structural properties of the polymer chains in the interface.

III. Results and Discussion

III.1. Structural Results. In this section we examine the predictions of the lattice model for the density profiles of end segments as a function of the different parameters, namely r and χ_s, which characterize these systems. These results are qualitatively in agreement with Monte Carlo results discussed in Appendix A. Figure 1a is a plot of the volume fraction of end groups, $\Phi_{1,i}$, as a function of the lattice layer number, i, for a chain of length $r = 10$ over a range of χ_s values. The depth of the layer from the surface, z, can be calculated as the number of lattice layers times the lattice dimension, or more precisely in the present case of a cubic lattice of volume v_e, $z = i(v_e)^{1/3}$. Figure 1b is the corresponding plot for $r = 100$. A few general trends can be observed in both cases. First, for positive values of χ_s, the end group fraction in the immediate vicinity of the surface is less than that in the bulk. For a given chain length, this depletion increases with χ_s. Following this depletion, there is an enhancement of ends in subsequent layers so as to conserve the total number of chain ends in the interfacial layer. The width of the interfacial layer scales with the unperturbed radius of gyration of the molecules in question.[21] These trends reverse when one considers negative values of χ_s, in that there is an enhancement of end groups in the immediate vicinity of the surface, followed by a depletion layer and a gradual gradient back to the bulk concentration. It is interesting to note that the direct surface interaction appears to be confined to the first lattice layer. This result is consistent with the concept of bulk screening.

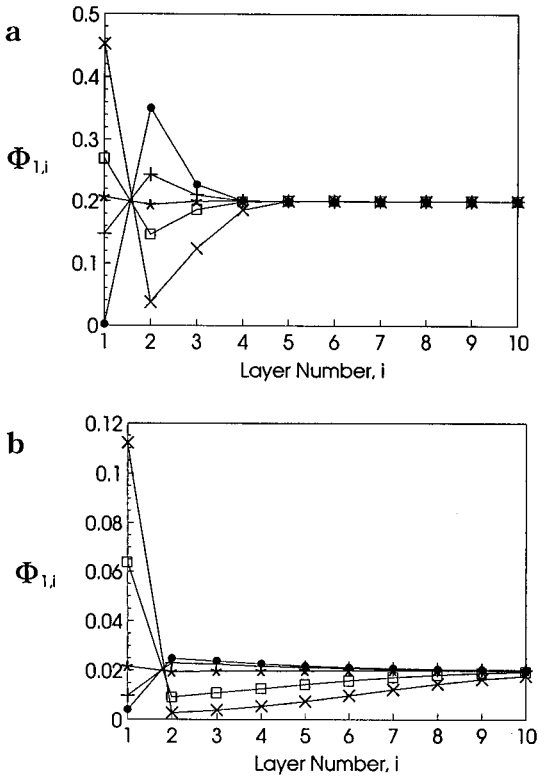

Figure 1. End group volume fractions as a function of the lattice layer number, i, as calculated from the lattice model. The distance from the surface, z, is related to the lattice layer number by $z = i(v_e)^{2/3}$, where v_e is the volume of the lattice site (i.e., the end group). (a) $r = 10$: the different symbols correspond to $\chi_s = 4$ (●), $\chi_s = 1$ (+), $\chi_s = 0$ (*), $\chi_s = -1$ (□), $\chi_s = -4$ (×). (b) $r = 100$ for $\chi_s = 2$ (●), $\chi_s = 1$ (+), $\chi_s = 0$ (*), $\chi_s = -1$ (□), $\chi_s = -2$ (×). The lines are guides to the eye.

In this context, we note that the experimentally determined density profiles[14,23] of the end groups show oscillations that persist beyond the first "wave" that is observed in Figure 1. These additional oscillations are very reminiscent of the density profiles observed for

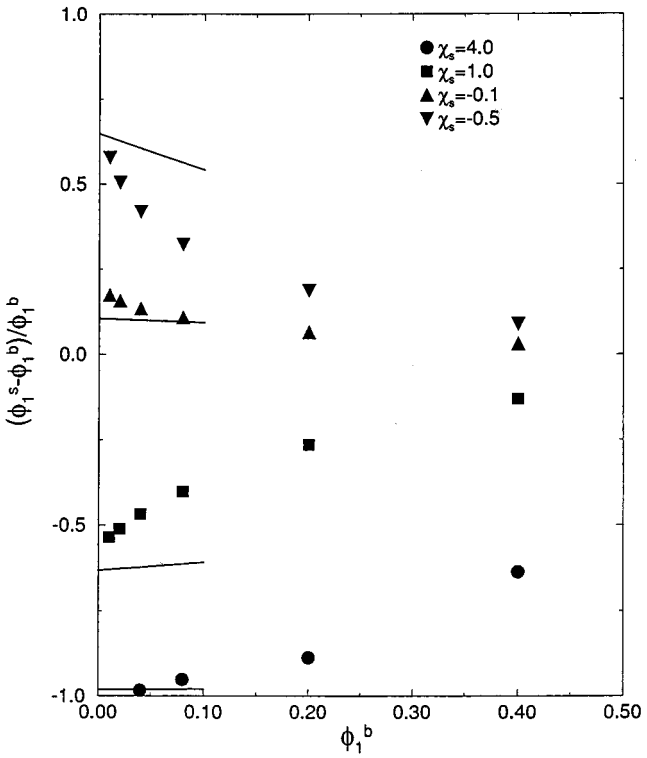

Figure 2. Plot of $(\phi_1^s - \phi_1^b)/\phi_1^b$ vs ϕ_1^b for different values of χ_s. The lines are predictions of (6).

disordered diblock and triblock copolymers near the order−disorder transition in the vicinity of a surface and are manifestations of the partial miscibility of the end groups with the middle moieties.[17,24,25] The theoretical results following the Scheutjens−Fleer model do not show additional oscillations since we have artificially set the value of the bulk interaction parameter between the end group and repeat unit segments, χ, to be equal to zero. This conclusion has also been verified by the off-lattice Monte Carlo simulations discussed in Appendix A. Further, it is important to stress that calculations for triblock copolymers using the same lattice formalism, but with finite χ values between the end group and repeat unit segments, do show oscillatory profiles similar to those observed experimentally.[17]

We now reconsider the data in Figure 1 and examine the volume fraction of end groups at the surface, ϕ_1^s, as a function of the bulk volume fractions of end groups in the system (i.e., $\phi_e = \phi_1^b = 2/r$). Note that the surface volume fraction is simply given by the composition of the first lattice layer (i.e., $\phi_i^s \equiv \Phi_{i,1}$). We start with the assumption that entropic effects play only a relatively minor role in determining the segregation of end groups to the surface. The validity of this assumption will be tested below. Consequently, the free energy change associated with replacing an end group at the surface with a repeat unit segment is $-\chi_s k_B T$. Based upon standard partitioning ideas, the volume fraction of end groups in the immediate vicinity of the surface is given by the expression

$$\phi_1^s = \frac{\phi_1^b e^{-\chi_s}}{1 - \phi_1^b + \phi_1^b e^{-\chi_s}} \tag{5}$$

where it is important to stress that we have ignored all connectivity effects (and the related entropic factors) and assumed that segregation effects are driven purely by surface energy differences between the end group and repeat unit segments.

Table 1. Lattice Model Predictions for End Group Fractions in the First Lattice Layer (i.e., at the Surface)

	$r = 5$	$r = 10$	$r = 25$	$r = 50$	$r = 100$	$r = 200$
$\chi_s = -4.0$	0.673	0.452	0.262	0.172	0.112	0.0725
$\chi_s = -2.0$	0.530	0.333	0.175	0.106	0.064	
$\chi_s = -1.0$	0.466	0.269	0.129	0.073	0.041	
$\chi_s = -0.5$	0.435	0.237	0.106	0.057	0.030	0.016
$\chi_s = -0.25$	0.421	0.222	0.095	0.050	0.026	
$\chi_s = -0.1$	0.412	0.213	0.089	0.045	0.023	0.012
$\chi_s = 0$	0.406	0.207	0.085	0.043	0.022	0.011
$\chi_s = 0.1$	0.401	0.201	0.080	0.043	0.022	0.011
$\chi_s = 0.25$	0.392	0.192	0.074	0.037	0.018	0.0088
$\chi_s = 0.5$	0.378	0.177	0.065	0.031	0.015	0.007
$\chi_s = 1.0$	0.348	0.147	0.048	0.021	0.010	0.005
$\chi_s = 2.0$	0.285	0.093	0.023	0.009	0.004	
$\chi_s = 4.0$	0.145	0.023	0.004	0.001		

For a given value of χ_s and for long chains, (5) can be reduced to the form

$$\frac{\phi_1^s - \phi_1^b}{\phi_1^b} \approx (e^{-\chi_s} - 1)(1 - e^{-\chi_s}\phi_1^b) \tag{6}$$

In Figure 2 (see Table 1 for raw data) we plot this normalized end group fraction in the immediate vicinity of the surface as obtained from the lattice calculations at four different values of χ_s to test for the validity of this approximate form, (6). The chain end segregation, for each value of χ_s, approaches its asymptotic infinite chain length value with a linear dependence on ϕ_1^b, as expected by this equation. However, the predictions of (6) are only qualitatively in agreement with the data, thus illustrating that the neglect of entropic effects causes quantitative inaccuracies in determining the chain length dependence of end group segregation.

Further, the segregation of chain ends for the two longest chain lengths for moderate values of χ_s can be collapsed, especially if they are plotted by a form dictated by (5),

$$\chi_s = -\ln\left\{\frac{r-2}{2}\frac{\phi_1^s}{1-\phi_1^s}\right\} \tag{7}$$

Note that the right hand side of (7) simply reduces to the ratio of the surface to bulk volume fraction of chain ends, ϕ_1^s/ϕ_1^b, in the limit of long chains. As shown in Figure 3 (see Table 1 for raw data), a plot of the two sides of this equation fall approximately along a 45° line,[26] thus illustrating that energetic effects apparently dominate the partitioning of chain ends to the surface and that entropic effects play a minor, but not a trivial, role in this context.

In summary, we have shown here that the partitioning of chain end groups to or away from a surface can be understood qualitatively by ignoring the effects of chain connectivity and thus treating the system as being a dilute gas of chain end groups being driven to the surface through energy considerations alone [see (5)]. While this provides a reasonable first approximation to the essential physics in this problem, it is important to emphasize that entropic effects, which prefer the placement of chain ends at the surface even for athermal systems, have to be considered to obtain a quantitative understanding of the partitioning of chain ends to the surface.

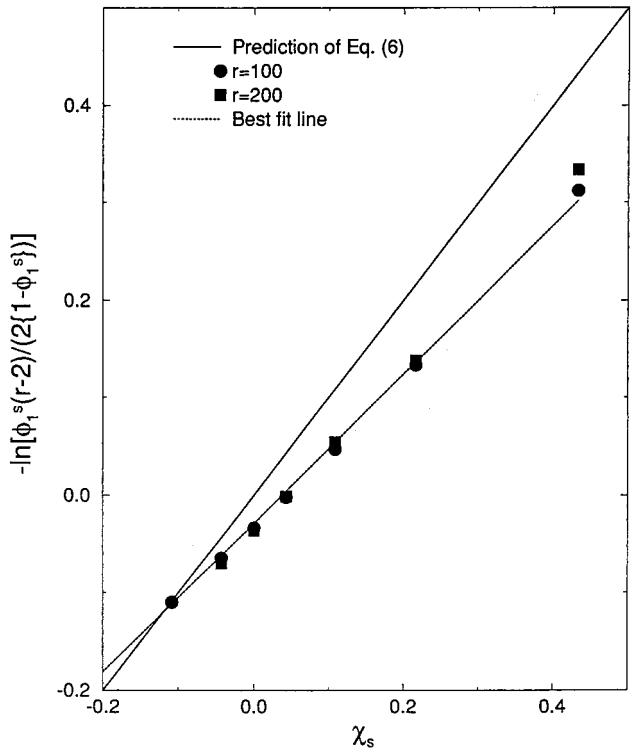

Figure 3. Plot of $-\ln\{\phi_1^s(r-2)/[2(1-\phi_1^s)]\}$ vs χ_s for chains of length $r = 100$ and 200, respectively. The continuous line is a prediction of (7), while the dashed line is a best fit.

III.2. Comparison of Predicted Surface Tensions with Experiment. The primary quantities of interest in this work are the surface tensions of end-functional PDMS melts as a function of their number average molecular weight, M_n (or, alternatively, their normalized chain length r).[8] Before we consider an end-functional system, it is instructive to examine the Scheutjens−Fleer predictions for the closely related problem of determining the surface tension of a binary polymer blend in the hypothetical incompressible limit. We consider eq 25 from ref 21 in the limit where $\chi = 0$ and write to leading order that

$$\frac{\gamma a}{k_b T} = \phi_1^s\left[\frac{\gamma a}{k_B T}\right]_1 + (1-\phi_1^s)\left[\frac{\gamma a}{k_B T}\right]_2 \qquad (8)$$

where $[\gamma a/k_B T]_i$ is the normalized surface tension of a segment of type i and a is the area occupied by that segment at the surface. The subscripts 1 and 2 denote the two different blend components. We have assumed in the derivation of this approximate relation that only segments in the first lattice layer contribute to the surface tension, and consequently, we have ignored any contributions arising from other layers. While this may appear, in general, to be a poor theoretical approximation, it is numerically very reliable, as has been illustrated by our past work on polymer blends in the vicinity of hard surfaces.[21] This equation is extremely useful in the context of this paper, since it suggests that the surface tension of end-functional polymer chains will be a linear combination of the surface tensions of the end group and repeat unit segments, with the appropriate weighting being the surface composition of the two segments. Note that this approximation effectively assumes that chain connectivity only affects the volume fractions of the two components at the surface and does not contribute additionally to the surface tensions (e.g., through an entropic effect).

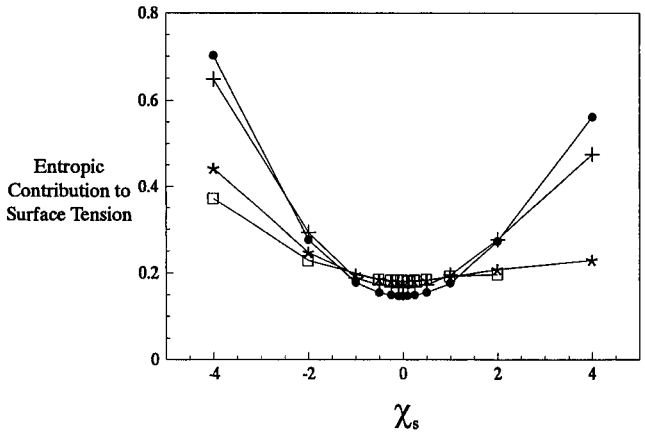

Figure 4. Plot of the dimensionless entropic contribution to the surface tension as a function of χ_s for different chain lengths: (●) $r = 5$; (+) $r = 10$; (*) $r = 50$; (□) $r = 100$.

To lend credence to this picture, we have considered the exact surface tensions, which include entropic and energetic effects, of the end-functional polymers of interest in this work through the device of the Scheutjens−Fleer incompressible lattice model.[16,17] In Figure 4 we consider only the entropic contribution to the surface tension as a function of χ_s for four different chain lengths. For moderate χ_s values ($-2 < \chi_s < 2$), it is immediately apparent that, although the entropic contribution is non-zero, it effectively remains unchanged over a broad range of chain lengths and surface energy differences. Consequently, while connectivity effects play an important role in determining the chain length dependence of the *segregation* of chain ends to the surface, the corresponding entropic effects, which arise from the modification of chain conformations near the surface, *do not* appear to play a critical role in determining the chain length dependence of surface tensions.

Comparison of the theoretical predictions with experimental surface tension data requires the knowledge of only two experimental parameters, the normalized chain length, r, defined by (2) and the surface interaction parameter, χ_s, defined by

$$\chi_s = \frac{(\gamma_e - \gamma_r)a}{kT} \qquad (9)$$

where the subscripts e and r refer to the end group and repeat unit segments, respectively. In using (9), we take a as the projected area of a lattice site. Since the end group volume has been selected as the reference for definition of the lattice size and the normalized chain length, it follows that $a = (v_e)^{2/3}$. Once experimental values for the two parameters are obtained, the surface composition can be calculated from the lattice theory. In the case where projected surface areas are equal, (8) reduces to

$$\gamma = \gamma_e\phi_e^s + \gamma_r\phi_r^s \qquad (10)$$

Note again that the surface volume fraction is simply given by the composition in the first lattice layer (i.e., $\phi_i^s \equiv \Phi_{i,1}$).

The theory can be compared to experimental surface tensions measured for α,ω-functional poly(dimethylsiloxanes).[8] The chemical structure of the polymers is symmetric, as represented schematically in Figure 5, due to the synthetic procedure used for their polymer-

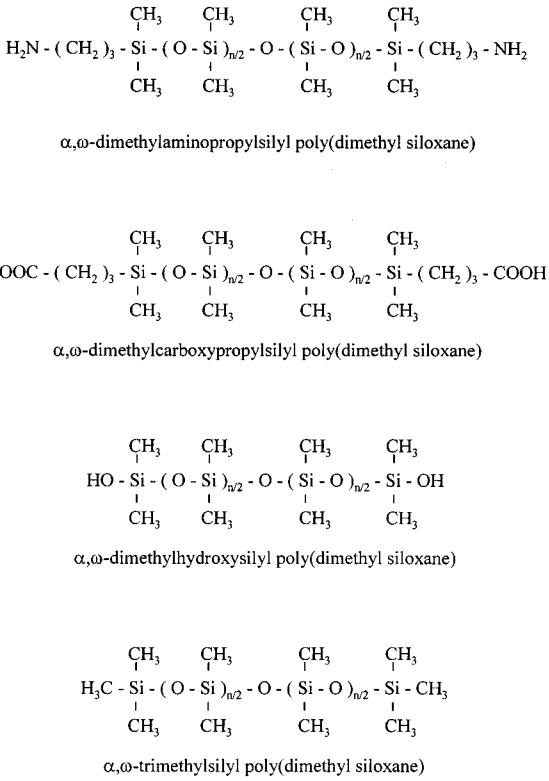

Figure 5. Schematic structures of α,ω-functional poly(dimethylsiloxanes).

ization. The schematic furnishes an obvious definition of the structure of the end group. Surface tensions have been measured for four different end groups: trimethylsilyl [methyl], dimethylhydroxylsilyl [hydroxyl], dimethyl(aminopropyl)silyl [amino], and dimethyl(carboxypropyl)silyl [carboxyl], where the names in brackets denote the nominal functionality of the end group. The measurements of the first three systems have been reported previously,[8] while measurements on the carboxyl system have been made specifically for the current work using the previously described methods.

The volumes of the repeat units and end groups as defined in this fashion are determined from experimental measurements of the density,[8] as detailed in Appendix B. The calculations thereby account properly for the dependence of bulk density on end group type and molecular weight, as shown in Figure B1 in Appendix B. The surface tension values for the end group and repeat unit segments are determined by group additivity methods[8,24] that are also described in Appendix B. Table 2 contains a summary of experimentally determined segment volumes and projected surface areas, as well as the results of solubility parameter, surface tension, and surface interaction parameter calculations.

The surface tensions predicted from this self-consistent approach are compared to experimental data for PDMS with the four different end groups in Figures 6−9. For comparisons sake, calculations neglecting any segregation of end groups [i.e., where the surface compositions in (10) are set equal to the bulk compositions; $\phi_e = 2/r$] are also presented. As can be seen, there is excellent agreement between experiment and the results of these simple calculations, suggesting that the essential physics of the situation are embodied in the determination of the surface composition of the end group and repeat unit segments in the immediate vicinity of the surface (i.e., in the first lattice layer). It should be emphasized that there are no adjustable

Table 2. Summary of Parameters Used in Calculations for End-Functional PDMS Chains

	segment				
parameter	methyl	amine	hydroxyl	carboxyl	backbone
volume (cm^3/mol)	102.23	127.8	75.31	139.2	76.59
a (nm^2)	0.307	0.356	0.250	0.377	0.253
δ_{disp}	5.91	7.95	8.18	8.56	6.01
δ_{polar}	0	1.43	3.29	1.50	1.91
γ_{PDMS}(eq B.7) (dynes/cm)	n.a.	n.a.	n.a.	n.a.	20.91
γ_{PDMS}(exptl) (dynes/cm)	n.a.	n.a.	n.a.	n.a.	20.40 ± 0.07
$\gamma_{H\&S}$(eq B.8) (dynes/cm)	11.66	22.75	20.19	27.16	n.a.
$\gamma_{K\&S}$(eq B.9) (dynes/cm)	11.83	23.82	23.79	28.39	n.a.
$\chi_{s,H\&S}$[a]	−0.640	0.200	−0.012	0.610	
$\chi_{s,K\&S}$[b]	−0.628	0.291	0.203	0.720	

[a] Calculated from (9) using the $\gamma_{PDMS} = 20.4 \pm 0.07$ dynes/cm and $\gamma_{H\&S}$ for the end group. [b] Calculated from (9) using the $\gamma_{PDMS} = 20.4 \pm 0.07$ dynes/cm and $\gamma_{K\&S}$ for the end group.

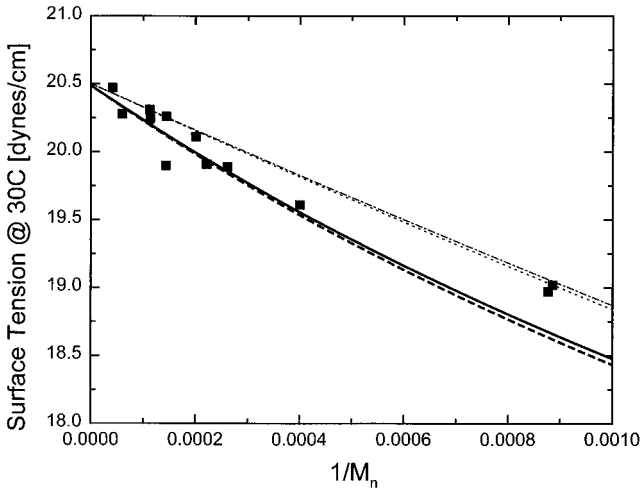

Figure 6. Experimental (symbols) and theoretical results for the variation of surface tensions of α,ω-trimethylsilyl-PDMS chains with chain length. The thick solid line denotes the full theoretical prediction utilizing Koenhen and Smolders (K&S) (B.9) to calculate the solubility parameter of the end group; the thick dashed line denotes the full theoretical prediction utilizing Hildebrand and Scott (H&S) (B.8) to calculate the solubility parameter of the end group. The thin dash-dot-dash line is the calculation using K&S but neglecting surface segregation (i.e., $\phi_e^s = 2/r$), and the thin dotted line is the calculation using H&S but neglecting surface segregation.

parameters used in these comparisons. The deviation between theory and experiment is well within the errors involved with estimation of surface tensions from group contribution methods. In most cases studied, there is little difference between the full calculation and the calculation that neglects surface segregation altogether. This result is consistent with the data in Table 1 that show that surface segregation becomes prominent only for large values of χ_s. The systems studied have relatively small values for this parameter, listed in Table 2. The primary effect that leads to the molecular weight dependence of surface tension is therefore the direct dependence of bulk end group concentration on chain length, represented by $\phi_e = 2/r$ incorporated into (10).

The simple approach developed herein can be readily employed to predict surface tensions for other end-functional polymers by following the following procedure. First, the volumes of the end groups must be

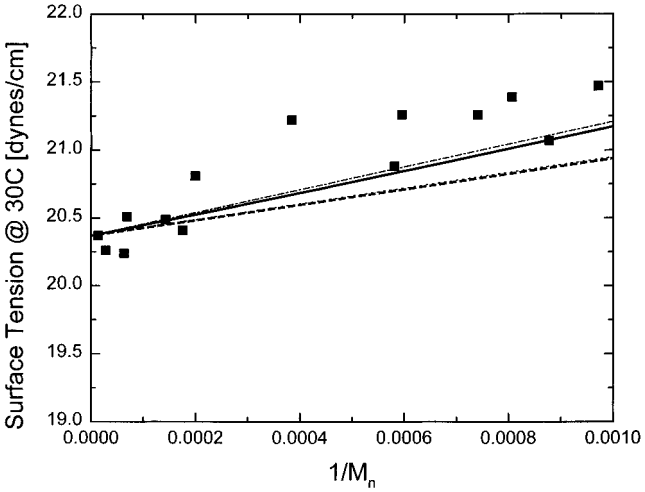

Figure 7. Experimental (symbols) and theoretical results for the variation of surface tensions of α,ω-dimethyl(aminopropyl)-silyl-PDMS chains with chain length. The thick solid line denotes the full theoretical prediction utilizing K&S (B.9) to calculate the solubility parameter of the end group; the thick dashed line denotes the full theoretical prediction utilizing H&S (B.8) to calculate the solubility parameter of the end group. The thin dash-dot-dash line is the calculation using K&S but neglecting surface segregation (i.e., $\phi_e^s = 2/r$), and the thin dotted line is the calculation using H&S but neglecting surface segregation.

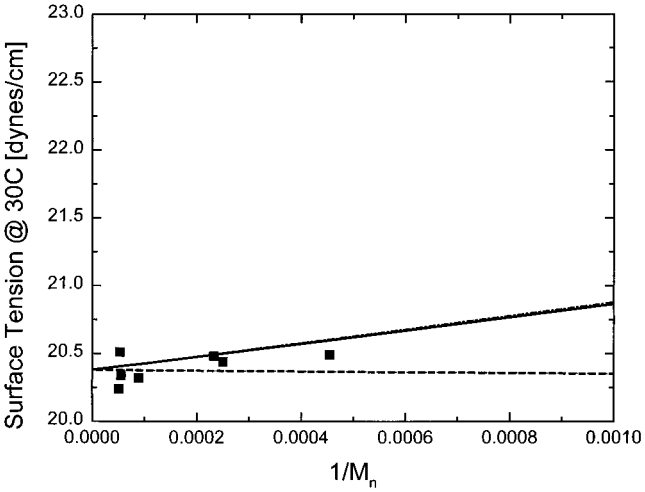

Figure 8. Experimental (symbols) and theoretical results for the variation of surface tensions of α,ω-dimethylhydroxysilyl-PDMS chains with chain length. The thick solid line denotes the full theoretical prediction utilizing K&S (B.9) to calculate the solubility parameter of the end group; the thick dashed line denotes the full theoretical prediction utilizing H&S (B.8) to calculate the solubility parameter of the end group. The thin dash-dot-dash line is the calculation using K&S but neglecting surface segregation (i.e., $\phi_e^s = 2/r$), and the thin dotted line is the calculation using H&S but neglecting surface segregation.

determined experimentally or estimated by group additivity methods. Once the volumes are known, the solubility parameters and surface tensions for the end group and repeat unit segments can be calculated according to the group additivity relations presented in Appendix B. If the reference volume is set to the volume of the chain end, the segment surface area can be determined from $a = (v_e)^{2/3}$, and the surface interaction parameter, χ_s, can be calculated according to (9). Once χ_s is known, the end group surface composition can be determined for various normalized chain lengths from Table 1. At fixed normalized chain lengths, the relationship between surface composition and χ_s is well

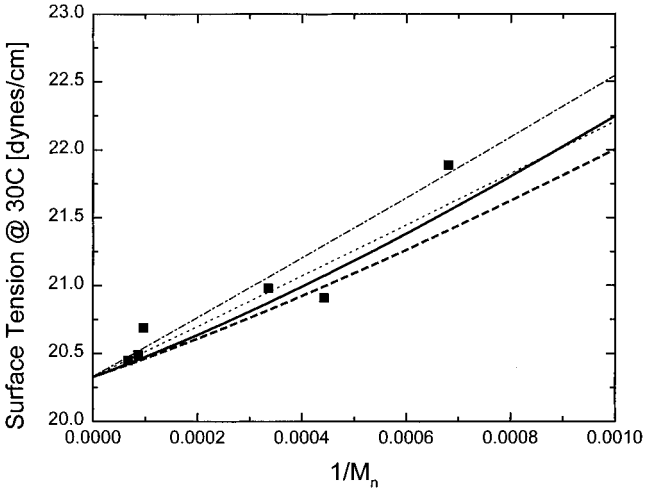

Figure 9. Experimental (symbols) and theoretical results for the variation of surface tensions of α,ω-dimethyl(carboxypropyl)silyl-PDMS chains with chain length. The thick solid line denotes the full theoretical prediction utilizing K&S (B.9) to calculate the solubility parameter of the end group; the thick dashed line denotes the full theoretical prediction utilizing H&S (B.8) to calculate the solubility parameter of the end group. The thin dash-dot-dash line is the calculation using K&S but neglecting surface segregation (i.e., $\phi_e^s = 2/r$), and the thin dotted line is the calculation using H&S but neglecting surface segregation.

characterized by a quadratic function, and thus interpolation for χ_s values that do not appear in the table is readily accomplished by a quadratic fit to the data for each column in Table 1. For ease of applicability, we have included the results of quadratic regressions to the surface composition vs χ_s data (Table 1 at fixed chain length) in Appendix C. The surface tension for the molecule is then calculated from the surface composition and estimated surface tensions by application of (10), and the actual molecular weight can then be determined for the particular normalized chain length by application of (2) and a knowledge of the molecular weights of the repeat unit and end group segments.

One advantage to the theoretical framework presented herein is that chains of a variety of different architectures (e.g., combs, stars, etc.) can also be modeled using a similar approach to develop a table of surface compositions as a function of χ_s for that particular architecture. Once the table is available, the surface tensions can be calculated from the surface composition as described in the paragraph above.

IV. Conclusions

The major premise of this work is that the surface tensions of homopolymer chains can be altered significantly by the presence of end groups that are energetically favored or disfavored at a surface. The heuristic approach we have adopted here is to utilize the Scheutjens−Fleer incompressible self-consistent mean-field model to determine the partitioning of end groups from a polymer chain to a surface. The only input parameters required are the normalized chain length and a dimensionless surface interaction parameter related to the relative surface adsorption energies of the chain end and repeat unit. In the particular implementation utilized herein, the surface energy difference, χ_s, is derived from surface tension values for the end group and repeat unit segments estimated by group contribution methods. We then assume that all effects arising from the sharp density gradients present at the free

surface are incorporated into the group contribution estimates of surface tensions. With this approach the surface tension of the melt is equal to the weighted mean of the surface tensions of the two moieties, with the surface composition determining the weight given to the two different values. These simple ideas provide a nearly quantitative description of experimental surface tension data for α,ω-functional PDMS, suggesting that the surface composition of chain ends is indeed the critical variable in determining the unusual molecular weight dependence of the surface tensions for PDMS chains terminated with different end groups. The primary factor determining the dependence of surface tension on molecular weight is the direct relationship between the bulk end group concentration and chain length represented by $\phi_e = 2/r$. Segregation effects that influence the end group surface composition are enthalpically dominated and impact the molecular weight dependence of surface tension only for large χ_s. Entropic effects have a minimal impact on the molecular weight dependence. Through this approach we now have a self-consistent means to determine the surface segregation, as well as the surface tensions of end-functional polymers, as long as one has group contribution methods to determine the surface tensions of the end groups and repeat units of interest.

Acknowledgment. Financial support for this work at Penn State University was provided by the National Science Foundation (CTS-9311915). The University of Connecticut researchers acknowledge support from the National Science Foundation Polymer Program (DMR-8818232 and DMR 9502977), the Office of Naval Research, and the U. S. Army Research Office.

Appendix A: Monte Carlo Simulations

In parallel with the lattice calculations, we have also conducted off-lattice Monte Carlo simulations to examine the accuracy of the lattice model in describing the structure of the chain molecules in the interface. The results of this investigation are reported below.

A.1. Model Description. The polymer molecules are modeled as chains of tangentially connected spheres of diameter σ. Since all nonbonded beads interact with the same 6−12 Lennard-Jones potential,[27]

$$U(r_{ij}) = 4\epsilon\left[\left(\frac{\sigma}{r_{ij}}\right)^{12} - \left(\frac{\sigma}{r_{ij}}\right)^{6}\right] \qquad r_{ij} < 2.5\sigma \quad \text{(A.1)}$$

$$= 0, \text{ otherwise}$$

the χ parameters between the end and repeat unit segments are effectively set to zero. Here U describes the energy of interaction between two beads separated by a distance of r_{ij}, and ϵ and σ represent the parameters in the Lennard-Jones model. The walls were considered to be impenetrable to the centers of all of the beads in the system. In addition to this hard repulsion condition, the end beads on the chains interacted with the walls through a potential of the form

$$U_{wall}(z) = \frac{\epsilon_w}{(z/\sigma + 0.5)^3} \quad \text{(A.2)}$$

The sign and the magnitude of the constant ϵ_w dictates the strength of the wall−end group potential. Both positive and negative values of this parameter have been considered in these simulations.

The simulation cell is a rectangular parallelepiped bounded by parallel infinite hard walls (which are impenetrable to the centers of sites of the polymer molecules) in the z-direction at a separation $H\sigma$. We are interested in the segregation of the chain ends to these hard walls. Periodic boundary conditions are imposed along the other two (x and y) directions with a box length of $L\sigma$ along each coordinate. H and L were both set to a value of 10.55 in these simulations. The degree of polymerization, r, was varied from 10 to 100 in a series of simulations, and the systems contained 800 monomers. The overall reduced density ($\rho \equiv N_M r/L^2H$ where N_M is the number of molecules) was set to 0.7 (characteristic of concentrated solutions or melts), and the temperature, $T^* \equiv k_BT/\epsilon$ was set to 2. All of the results that are reported here correspond to a single chain length of $r = 50$.

The initial states of the systems are generated randomly, ensuring chain connectivity, so that no two beads are closer than 0.8σ. The systems are then equilibrated following a Monte Carlo method with a combination of reptation and crank-shaft moves.[9] The systems are considered equilibrated when the density profiles are symmetric about the center of the film. Once the system is equilibrated, properties (including density profiles, order parameters, and the radius of gyration tensor) are averaged over 100−500 million attempted moves depending on the chain lengths and densities employed. Note that since the total density profiles of segments themselves are not uniform in this off-lattice system, we always normalize all of our end and middle segment densities by the total bead density at a z position so as to obtain the "volume fraction" profile of these species in the interface region.

A.2. Results. The primary results of our simulations relate to the normalized density profiles of the end segments in the immediate vicinity of the surface. In Figure A1 we consider a system of chains of length $r = 50$, where ϵ_w/k_BT assumed values of 0, 0.25, and 0.5, respectively. Except for the case of no repulsive interactions between the end groups and the wall, as shown in Figure A1, there is a depletion of chain ends in the immediate vicinity of the surface. Notice that we see only one oscillation in this density profile, exactly as has been observed in the lattice calculations, and this result is a direct manifestation of the fact that the interaction parameters between the chain ends and middle groups have been set to zero in these calculations.

In Figure A2 we consider the surface segregation for a chain system composed of chains of length $r = 50$, for a range of values of ϵ_w. The data are plotted exactly as in Figure 3, following (7), and in order to derive an appropriate value of χ_s, we note that the first shell in which we have recorded end densities is at $z \approx 0.1\sigma$. Consequently, we estimate that $\chi_s \approx \epsilon_w/(k_BT[0.6]^3)$. It can be seen clearly that the trends observed for the simulation results in Figure A2 closely parallel the trends observed in the lattice calculations, although we do not have a quantitative match on the slopes of the lines in the two cases. While this discrepancy can be attributed to the difficulty in mapping χ_s values from a free space calculation to a lattice situation, nevertheless, the lattice and off-lattice models are qualitatively in agreement for their predictions for the structures of polymer chains in this interfacial situation.

Appendix B: Group Contribution Calculations

The calculation of surface tension for end-functional polymers requires knowledge of the surface interaction

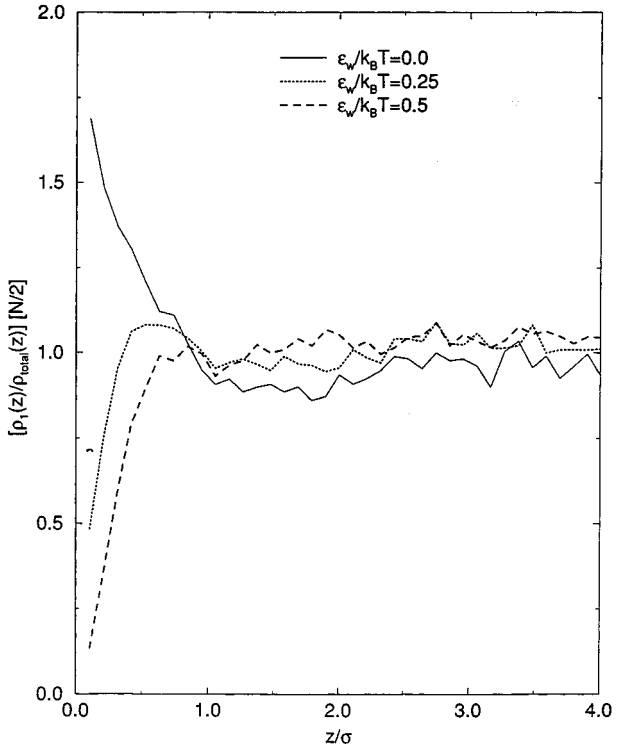

Figure A1. Monte Carlo simulation generated normalized end densities for chains of length $r = 50$ for three different values for the wall−end segment interaction potential, ϵ_w/k_BT, as a function of distance from the surface, z. Note that the end density, $\rho_1(z)$, at each point has been divided by the total bead density, $\rho_{total}(z)$. Further, this quantity has been scaled by the value expected in the bulk, i.e., $2/r$.

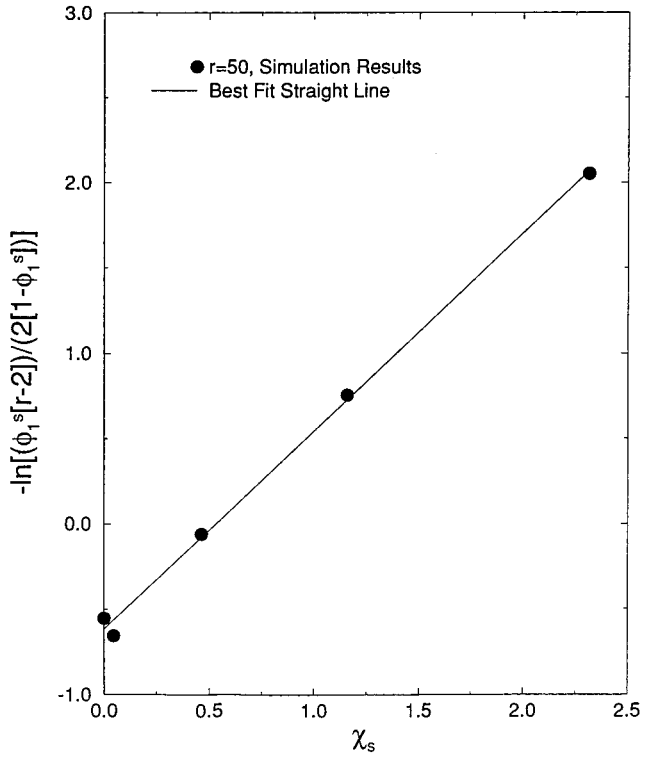

Figure A2. Values of normalized end density, $\phi_1^s \equiv \rho_1^s/\rho_{total}^s$, plotted in a form suggested by (7) and Figure 3.

parameter, χ_s, defined by

$$\chi_s = a(\gamma_e - \gamma_r)/k_BT \qquad (B.1)$$

where a is the surface area of a lattice site, k_B is the Boltzmann constant, T is temperature, and γ_i is the surface tension for component i. The surface tension of the polymer repeat unit, γ_r, can be measured by extrapolation of experimental surface tension values to infinite molecular weight. For poly(dimethylsiloxane) (PDMS),[8] this yielded a value of 20.37 ± 0.13 dynes/cm previously, but incorporation of the current data for carboxy-terminated PDMS gives a value of 20.40 ± 0.07 dynes/cm.

Table B1. Molar Attraction Constants

group	F_{disp}	F_{polar}
CH_3	214[30]	0
Si	−38[31]	0
CH_2	133[31]	0
OH	226[31]	248[32]
NH_2	227[32]	183[33]
COOH	403[32]	209[33]
O	70[31]	147[33]

The surface tension of the end group, γ_e, cannot be directly measured. An estimate of the end group surface tension can be made, however, by applying group additivity methods to calculate the solubility parameter of the end group and then by utilizing relations that describe how surface tension is related to the solubility parameters. The total solubility parameter, δ, is often described in terms of separable contributions due to dispersive (δ_{disp}), polar (δ_{polar}), and hydrogen-bonding (δ_{h-bond}) interactions:[28]

$$\delta^2 = (\delta_{disp})^2 + (\delta_{polar})^2 + (\delta_{h-bond})^2 \qquad (B.2)$$

Applying group contribution methods to each contribution, it follows that the three solubility parameters can be calculated from[29]

$$\delta_{disp} = \sum F_{i,disp}/v_m \qquad (B.3)$$

$$\delta_{polar} = \sum F_{i,polar}/v_m \qquad (B.4)$$

$$\delta_{h-bond} = \sum F_{i,h\text{-}bond}/v_m \qquad (B.5)$$

where v_m is the molar volume of the segment under consideration and $F_{i,disp}$, $F_{i,polar}$, and $F_{i,h-bond}$ are the molar attraction constants for dispersion-, dipole-, and hydrogen-bond forces, respectively.

Values for molar attraction constants necessary to calculate the solubility parameters of the PDMS backbone and the four different end groups employed in this study are contained in Table B1. Values are not presented for the hydrogen bonding contributions since these values are not employed in the calculation. The molar volumes required for these calculations can be obtained by analysis of experimental density (ρ) data.[8] Regression of a plot of $1/\rho$ vs $1/M_n$, where M_n is the number average molecular weight, yields values for the end group volume, v_e, and the repeat unit volume, v_r, since

$$1/\rho = (v_r/m_r) + 2(m_e v_r/m_r)\frac{1}{M_n} \qquad (B.6)$$

where m_r and m_e are the molecular weights of the repeat unit and end group, respectively. Density data for end-functional PDMS conform well to this relationship, as shown in Figure A1, and lead to the unit volumes shown in Table 2. The fact that these plots are linear demonstrates that volumes are additive and that the unit volumes obtained from the analysis are therefore partial

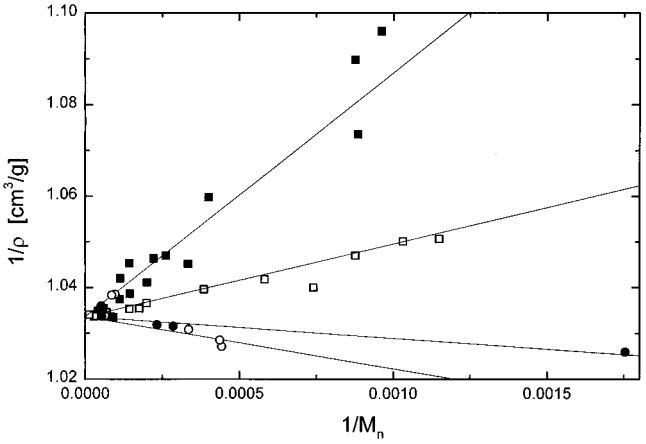

Figure B1. Variation of inverse density with inverse number average molecular weight. The solid lines show regression results for the data according to (B.6).

molar volumes; furthermore, they are independent of molecular weight.

A number of relationships are available[30] that relate the solubility parameters calculated from (B.3)−(B.5) (see Table 2) to the liquid surface tension. For polymers, the following relationship between δ_{disp} and surface tension has been proposed

$$\gamma_{disp} = (v_r/n_r)^{1/3}(\delta_{disp})^2/3.4 \qquad (B.7)$$

where n_r is the number of atoms in the repeat unit. Application of (B.7) to the PDMS backbone yields a surface tension of 20.9 dynes/cm, which compares favorably to the experimental value of 20.37 ± 0.13 dynes/cm reported previously[8] and the value of 20.40 ± 0.07 dynes/cm determined from the previous data including the new data on carboxylic acid-terminated PDMS. A myriad of similar relationships have been proposed for low molecular weight compounds. After evaluation of these in the current context, we have found two particular relationships that appear to give consistent results. The first of these was developed by Hildebrand and Scott[33] (H&S)

$$\gamma = 0.07147(\delta_{disp})^2(v_e)^{1/3} \qquad (B.8)$$

and the second was proposed by Koenhen and Smolders[30] (K&S)

$$\gamma = (\delta_{disp}{}^2 + \delta_{polar}{}^2)(v_e)^{1/3}/13.8 \qquad (B.9)$$

Solubility parameters of end groups calculated from (B.3) and (B.4), surface tension calculated from (B.7), (B.8) and (B.9), and subsequent surface interaction parameters calculated from (B.1) appear in Table 2.

Appendix C. Interpolation Procedure for Surface Composition Values of Table 1

The theoretical surface compositions listed in Table 1 are given only for a limited number of values of the surface interaction parameter, χ_s. We have found, however, that at fixed normalized chain length, r, the relationship between the surface composition, ϕ_1^s, and χ_s is well described by the following quadratic function:

$$\phi_1^s = a_0(r) + a_1(r)\chi_s + a_2(r)\chi_s{}^2 \qquad (C.1)$$

Table C1. Regression Parameters for Interpolation of Table 1

r	$a_0(r)$	$a_1(r)$	$a_2(r)$
5	0.4065	−0.0606	0.00027
10	0.2068	−0.0602	0.00153
25	0.0846	−0.0387	0.00362
50	0.0430	−0.0247	0.00364
100	0.02185	−0.0151	0.00305
200	0.0110	−0.0082	0.00179

The values of the three coefficients are listed as a function of the normalized chain length in Table C1.

References and Notes

(1) de Gennes P. G. *J. Phys. Paris* **1989**, *50*, 2551; *Can. J. Phys.* **1990**, *68*, 1049.
(2) Scheutjens, J. M. H. M.; Fleer, G. J. *J. Phys. Chem.* **1979**, *83*, 1619.
(3) Poser, C. I.; Sanchez, I. C. *J. Chem. Phys.* **1979**, *69*, 539.
(4) Wu, S. *Polymer Interface and Adhesion*; Marcel Dekker Inc.: New York, 1982.
(5) Bhatia, Q. S.; Chen, J.-K.; Koberstein, J. T.; Sohn, J. E.; Emerson, J. A. *J. Colloid Interface Sci.* **1985**, *106*, 353.
(6) Dee, G. T.; Sauer, B. B. *J. Colloid Interface Sci.* **1992**, *152*, 85.
(7) Sauer, B. B.; Dee, G. T. *Macromolecules* **1991**, *24*, 2124.
(8) Jalbert, C.; Koberstein, J. T.; Yilgor, I.; Gallagher, P.; Krukonis, V. *Macromolecules* **1993**, *26*, 3069.
(9) Kumar, S. K.; Vacatello, M.; Yoon, D. Y. *J. Chem. Phys.* **1988**, *89*, 5206; *Macromolecules* **1990**, *23*, 2189.
(10) Mansfield, K. F.; Theodorou, D. N. *Macromolecules* **1991**, *24*, 6283.
(11) Bitsanis, I.; Hadziioannou, G. *J. Chem. Phys.* **1990**, *92*, 3827.
(12) Yethiraj, A.; Hall, C. K. *Macromolecules* **1990**, *23*, 1865.
(13) de Gennes, P. G. *C. R. Acad. Sci., Ser. II* **1988**, *307*, 1841.
(14) Jalbert, C. J.; Koberstein, J. T.; Balaji, R. *Macromolecules* **1994**, *27*, 2409.
(15) Elman, J. F.; Koberstein, J. T.; Long, T. E. *Macromolecules* **1994**, *27*, 5341.
(16) Theodorou, D. N. *Macromolecules* **1988**, *21*, 1411.
(17) Hariharan, A.; Harris J. *J. Chem. Phys* **1994**, *101*, 3353.
(18) Hariharan, A.; Kumar, S. K.; Russell, T. P. *J. Chem. Phys.* **1993**, *98*, 6516; **1993**, *99*, 4041.
(19) Theodorou, D. N. *Lawrence Berkeley Lab., [Rep.] LBL* 1988.
(20) Kumar, S. K.; Russell, T. P; Hariharan, A. *Chem. Eng. Sci.* **1994**, *49*, 2899.
(21) Hariharan, A.; Kumar, S. K.; Russell, T. P. *Macromolecules* **1991**, *24*, 4909.
(22) Flory, P. J. *Principles of Polymer Chemistry*; Cornell University Press: Ithaca, NY, 1953.
(23) Jalbert, C. J. Ph.D. Thesis, University of Connecticut, 1993.
(24) Anastasiadis, S. H.; Russell, T. P.; Satija, S. K. *Phys. Rev. Lett.* **1989**, *62*, 1852.
(25) Fredrickson, G. H. *Macromolecules* **1987**, *20*, 2535.
(26) In fact the best fit to the lattice calculations shown in Figure 3 is given by the equation $y = 0.76x - 0.03$. This best fit straight line is shown in the figure to illustrate the importance of entropic effects in this context.
(27) Allan, M. P.; Tildesley, D. J *Computer Simulation of Liquids*; Clarendon Press: Oxford, New York, 1987.
(28) Hansen, C. M. *J. Paint Technol.* **1967**, *39*, 104.
(29) Koenhen, D. M.; Smolders, C. A. *J. Appl. Polym. Sci.* **1975**, *19*, 1163.
(30) *Handbook of Chemistry and Physics*; Weast, R. C., Ed.; CRC Press, Inc.: Cleveland, OH, 1975.
(31) Brandrup, J.; Immergut, E. H. *Polymer Handbook*, 3rd Ed.; John Wiley and Sons: New York, 1989.
(32) Estimated from the data in Table 1 in ref 30.
(33) Hildebrand, J. H.; Scott, R. L. *Solubility of Nonelectrolytes*; D. Van Nostrand: Princeton, NJ, 1950.

MA960224V